

# Single-platelet nanomechanics measured by high-throughput cytometry

David R. Myers<sup>1,2,3,4,5</sup>, Yongzhi Qiu<sup>1,2,3,4,5</sup>, Meredith E. Fay<sup>1,2,3,4,5</sup>, Michael Tennenbaum<sup>6</sup>, Daniel Chester<sup>7,8</sup>, Jonas Cuadrado<sup>6</sup>, Yumiko Sakurai<sup>1,2,3,4,5</sup>, Jong Baek<sup>1,2,3,4,5</sup>, Reginald Tran<sup>1,2,3,4,5</sup>, Jordan Ciciliano<sup>1,2,3,4,5</sup>, Byungwook Ahn<sup>1,2,3,4,5</sup>, Robert Mannino<sup>1,2,3,4,5</sup>, Silvia Bunting<sup>9</sup>, Carolyn Bennett<sup>1</sup>, Michael Briones<sup>1</sup>, Alberto Fernandez-Nieves<sup>4,6</sup>, Michael L. Smith<sup>10</sup>, Ashley C. Brown<sup>7,8</sup>, Todd Sulchek<sup>11</sup>, Wilbur A. Lam<sup>1,2,3,4,5</sup>

<sup>1</sup> Department of Pediatrics, Division of Pediatric Hematology/Oncology, Aflac Cancer Center and Blood Disorders Service of Children's Healthcare of Atlanta, Emory University School of Medicine, Atlanta, GA 30322

<sup>2</sup> The Wallace H. Coulter Department of Biomedical Engineering, Georgia Institute of Technology & Emory University, Atlanta, GA, 30332

<sup>3</sup> Winship Cancer Institute of Emory University, Atlanta, GA, 30322

<sup>4</sup> Parker H. Petit Institute of Bioengineering and Bioscience, Georgia Institute of Technology, Atlanta, GA 30332

<sup>5</sup> Institute for Electronics and Nanotechnology, Georgia Institute of Technology, Atlanta, GA 30332

<sup>6</sup> School of Physics, Georgia Institute of Technology, Atlanta, GA, 30332

<sup>7</sup> Joint Department of Biomedical Engineering, North Carolina State University and University of North Carolina at Chapel Hill, Raleigh, NC 27695

<sup>8</sup> Comparative Medicine Institute at North Carolina State University, Raleigh, NC 27695

<sup>9</sup> Department of Pathology, Emory University School of Medicine, Atlanta, GA 30322

<sup>10</sup> Department of Biomedical Engineering, Boston University, Boston, MA, 02215

<sup>11</sup> George W. Woodruff School of Mechanical Engineering, Georgia Institute of Technology, Atlanta, GA, 30332

## Supplementary Information

### Device design: Mechanics

#### Surface traction force microscopy

By constraining lithographically patterned arrays of fluorescently tagged proteins to a polyacrylamide gel surface, the computational and experimental constraints of traditional traction force microscopy are greatly reduced<sup>29</sup>. As cells adhere and move protein microdots, the independent traction force,  $\mathbf{T}$ , is calculated as:

$$\mathbf{T} = \frac{2\pi G a \mathbf{u}}{2 - \nu}$$

where  $G$  is the shear modulus,  $a$  is the microdot radius,  $\nu$  is Poisson's ratio, and  $\mathbf{u}$  is the displacement vector. By measuring the displacement of the microdot relative to the starting

position, the applied force is calculated. Since the shear modulus of polyacrylamide gels may be changed by changing the ratios of the precursor materials<sup>33</sup>, the mechanical stiffness felt by the platelet may be changed independent of other parameters such as the ligand area and density.

### **Simplification of traction force microscopy with two microdot system**

Noting that in fibrin clots, platelets may span and pull together two surfaces (Supplementary Figure 1), the method above may be simplified even further by spatially separating microdots such that platelets preferentially attach to two microdots (Supplementary Figure 2). Here, since the gel stiffness is constant, each microdot may be treated as a spring of equivalent stiffness,  $k$ , displaced from an equilibrium position  $u_1$  or  $u_2$ , as long as the microdot areas are approximately equal (Supplementary Figure 2). By static equilibrium,  $u_1 = u_2$ , and the displacement of each microdot is:

$$u_1 = u_2 = \frac{1}{2}(x_s - x_f)$$

where  $x_s$  is the starting distance of the microdots, and  $x_f$  is the final distance of the microdots. The traction force applied by the platelet is the sum of the applied traction forces and may be rewritten in terms of starting distance and final distance.

$$T = T_1 + T_2 = \frac{2\pi Ga u_1}{2 - \nu} + \frac{2\pi Ga u_2}{2 - \nu} = \frac{2\pi Ga}{2 - \nu}(x_s - x_f)$$

By rewriting the equations in this form, image post-processing is greatly simplified as only two measurements are needed: the final contracted distance and the original uncontracted distance.

Using this equation, the force as a function of pinch distance may be calculated for a variety of

different gel stiffnesses (Supplementary Figure 2). Due to the high precision lithography used here, the uncontracted distance may be assumed to be the distance of a neighboring unperturbed pair of microdots, and all measurements are performed once the experiment is completed.

### **Ligand size choice and spacing**

Using a micropatterning<sup>29</sup> approach to traction force microscopy, both ligand area, ligand density, and system stiffness could be independently controlled and tuned to mimic geometries and mechanical stiffnesses experienced in clots. In consideration of the platelet size and mindful of lithography and fabrication minimum feature size constraints, we created pairs of fibrinogen circular microdots with a radius of 0.8  $\mu\text{m}$ , and center to center distance of 4  $\mu\text{m}$  (Figure 1).

These numbers are similar to those seen in previous AFM studies showing that platelets spread to an area of approximately 1  $\mu\text{m}^2$  when pulling together two fibrinogen coated surfaces<sup>8</sup>, with microdot displacements of approximately 0.5 – 1  $\mu\text{m}$ . Such numbers also appeared to be in agreement with our own images of platelets contracting in fibrin gels (Supplementary Figure 1, Supplementary Video 1). By spacing pairs of microdots least 8  $\mu\text{m}$  apart<sup>8</sup>, platelet contraction was effectively confined to a single pair of microdots (**Error! Reference source not found.**)<sup>9</sup>.

The size of the microdots was an important parameter in confining the platelet interaction to two microdots. Platelets are less likely to span to a neighboring microdot when the microdot itself is large, whereas platelets may span many microdots if the microdots are small and closer together. Aside from creating an appropriate spatial geometry to interact with platelets, the microdot size is also appropriate for optical microscopy. Similarly, based on our force calculations, the microdot size is of an appropriate size to confer adequate force sensitivity and resolution. It is

important to note that since the microdot is also a signaling molecule for platelet contraction via  $\alpha_{IIb}\beta_3$ , that changes in the size could affect platelet behavior. However, any changes in platelet behavior due to a limited ligand area will be systemic since the ligand area is constant for all experiments. Moreover, the data is in agreement with previous atomic force microscopy studies<sup>8</sup>, which did not constrain ligand area. Also, since the ligand area also matches *in vitro* clot observations, any errors are expected to be minimal.

After establishing a system of appropriate spatial dimensions, we sought to ensure that the stiffness encountered by platelets was similar to those found in clots. At the single platelet level, this system is expected to be an analog for either platelet-platelet interactions or platelet-fibrin interactions, which are the primary interactions within a clot. A large variety of mechanical stiffnesses are encountered within clots, which have bulk elastic moduli between 45 – 70 Pa<sup>36</sup>. Activated contracted platelets have stiffness values of  $\sim 10$  kPa<sup>7</sup>; whereas individual fibrin fibers have stiffness values of 2 MPa (unligated) or 14.5 MPa (ligated)<sup>37</sup>. Using such values in conjunction with estimates for average fibrin fiber thickness and length, the mechanical stiffness and forces that platelets are likely to encounter within a clot may be estimated. Here the goal is to choose an appropriate range of PAA gel stiffnesses for use within our system. As such, these estimates will focus on limiting cases for the mechanical environment surrounding platelets. Several different approaches would be suitable for this analysis, but here, expected forces on platelets will be calculated and compared to values achievable with this system (Supplementary Figure 2)

For platelet-platelet interactions, two limiting cases are considered: when contracting platelets have free boundaries (Supplementary Figure 2) and when contracting platelets have fixed boundaries (Supplementary Figure 2). The free boundary case represents the softest interaction

which could be experienced by platelet-platelet interactions. In the simplified case, platelets are free to contract and will apply no force to do so. Practically, the material properties of individual platelets will play a dominant role in defining the stiffness of the system. Previous AFM studies have determined that activated, contracted platelets have stiffness of 10 kPa<sup>8</sup>. Hence, forces associated with such systems are expected to be low on the order of several nN. The fixed boundary case represents an interaction in an infinite stiffness environment, where platelets experience isometric contraction. Previous studies have already studied such cases and determined that contractile forces tend to maximum around 80 nN<sup>8</sup>. Our fibrinogen microdots must move in order for contraction to be measured, so PAA gel stiffnesses were chosen which would enable platelets to achieve similar forces with less than 1  $\mu\text{m}$  of contraction. Here, both 75 kPa and 100 kPa gel stiffness meet this criteria (Supplementary Figure 2).

For platelet-fibrin interactions, the limiting cases are defined by the direction in which a platelet pulls on a single fibrin strand, either perpendicular (Supplementary Figure 2) or parallel (Supplementary Figure 2). Using atomic force microscopy and fibrin fibers spanned across gaps, others have demonstrated that tension built in fibrin networks is through extension of the fibrin and not applied moments. Using published values<sup>37</sup> for typical ligated fibrin diameters ( $284 \pm 44$  nm), lengths ( $14.7 \pm 2.5$   $\mu\text{m}$ ), and modulus ( $14.5 \pm 3.5$  MPa), the forces associated with these two conditions may be estimated.

When the platelet pulls perpendicular to the fibrin strand the extension is minimal representing the limit of the soft mechanical environment. Here, assuming a 0.5  $\mu\text{m}$  platelet contraction, the strain,  $\epsilon$ , is then:

$$\epsilon = \frac{\Delta L}{L} = \frac{\sqrt{\delta^2 + L^2} - L}{20} = \frac{\sqrt{0.5^2 + 7.35^2} - 7.35}{7.35} = 0.0023$$

The associated angle is then:

$$\theta = \tan^{-1}\left(\frac{0.5}{7.35}\right) = 0.07$$

Due to symmetry in this system, and in consideration of static equilibrium, the force applied by the fibrin to the platelet is then:

$$F \sin \theta = E A \epsilon \sin \theta = (14.5 \text{ MPa}) \left(\frac{\pi}{4} (284 \text{ nm})^2\right) (0.0023) (\sin 0.07) = 0.15 \text{ nN}$$

When the platelet pulls the parallel to the fibrin strand, the extension is maximized. Assuming that the platelet is capable of pulling 0.5  $\mu\text{m}$ , the associated strain is then:

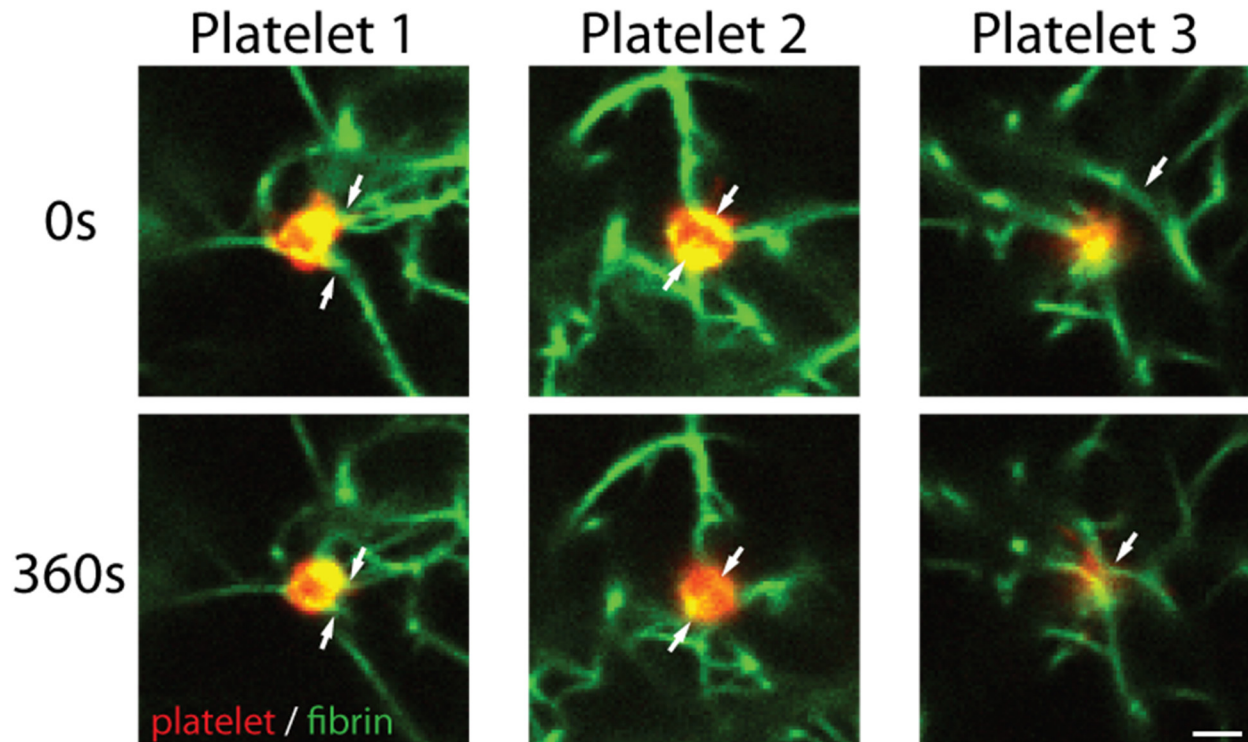
$$\epsilon = \frac{\Delta L}{L} = \frac{0.5}{14.7} = 0.034$$

The force is then

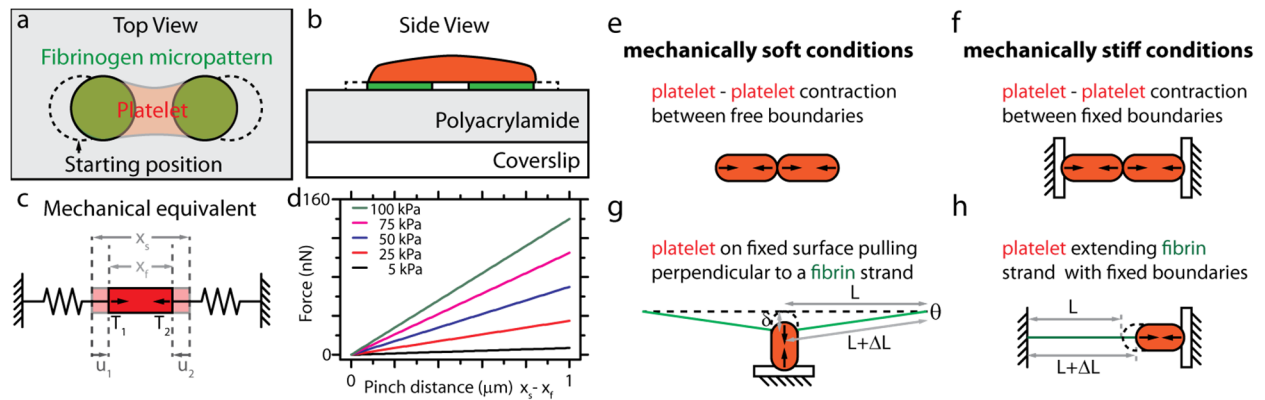
$$F = E A \epsilon = (14.5 \text{ MPa}) \left(\frac{\pi}{4} (284 \text{ nm})^2\right) (0.034) = 31 \text{ nN}$$

Also, if a platelet were pulling on unligated fibers in the developing clot (pre Factor XIII), then these values would be an order of magnitude lower. Hence, in examining these limiting cases and previously published values for platelet contraction, choosing PAA gels of stiffness between 5 and 100 kPa (Supplementary Figure 2) will adequately cover the micromechanical stiffness environment that a platelet will experience within a typical clot.

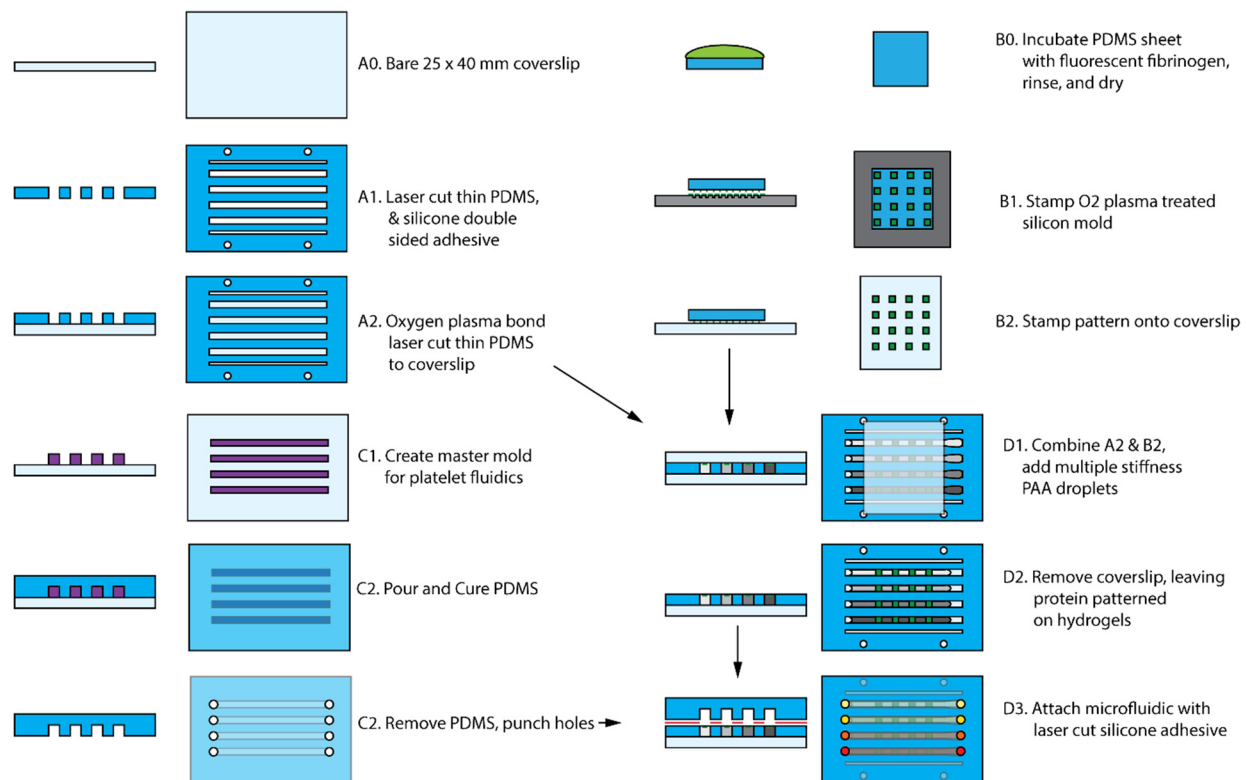
## Supplementary Figures



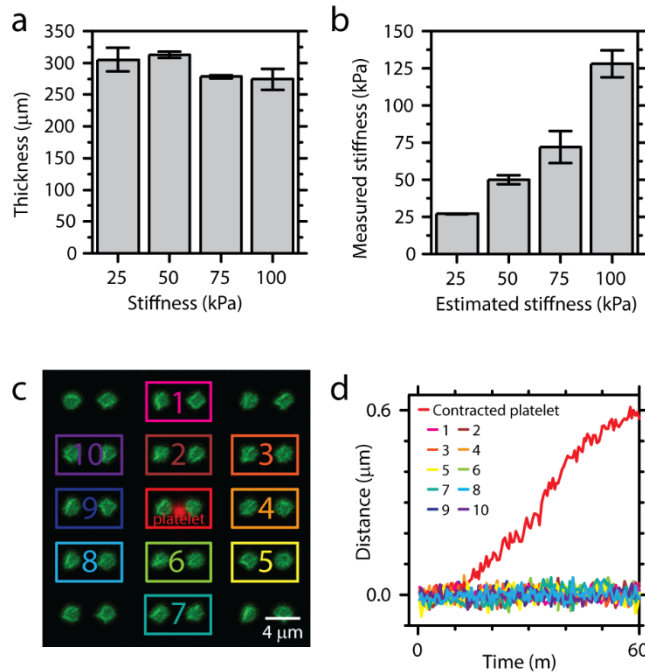
Supplementary Figure 1: Platelet contraction in 3d fibrin meshes span and pull adjacent fibers together of differing stiffness. The fibrin mesh has varying mechanical stiffness due to the differing thickness and cross linking point density. Here we show three platelets spanning fibrin filaments and pulling them together over the course of six minutes. White arrows point to same feature at both time points. Scale bar is 2  $\mu\text{m}$ .



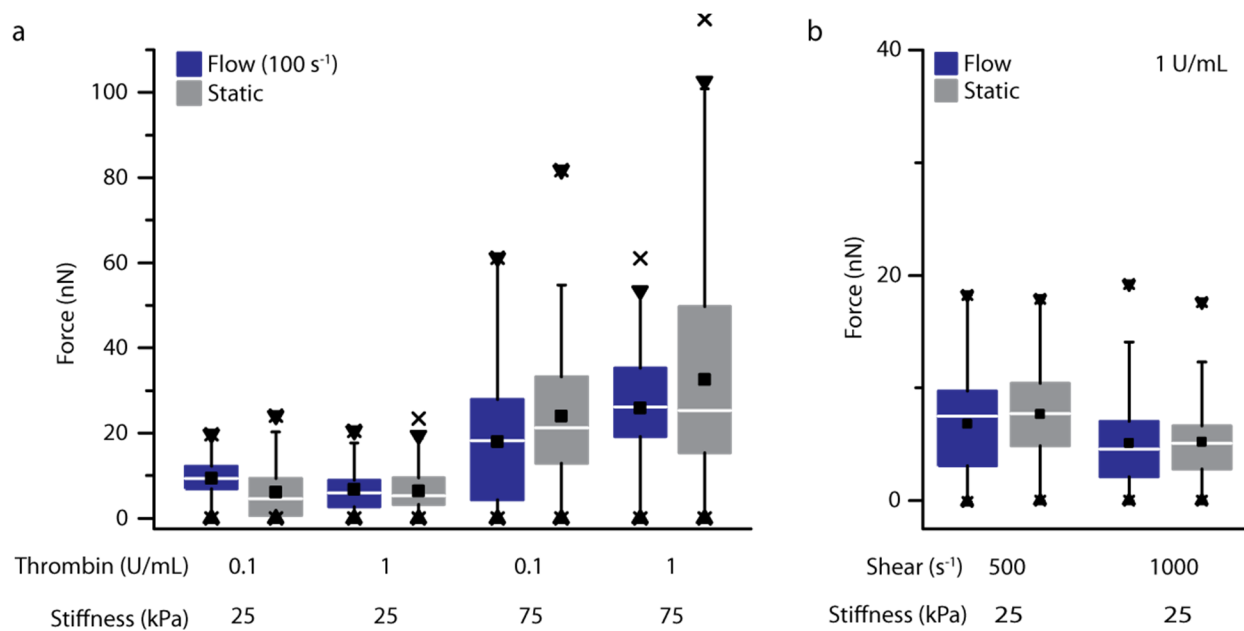
Supplementary Figure 2: Contractile system, mechanical model, and calculated forces as a function of pinch distance, and limiting cases for stiffness. **a-b**, The fibrinogen patches are covalently attached to the underlying hydrogel and move independently. **c**, Mechanically, this can be modeled as a platelet pulling on two springs of equivalent stiffness. **d**, The force a platelet will exert by pulling the fibrinogen patches together may be calculated from a measurement of the pinch distance for a range of different hydrogel stiffnesses. When considering force range, it is important to consider the limiting cases defining mechanical stiffness values **e**, Platelets contracting against one another with moving boundaries are expected to have stiffness on the order of 10 kPa, the value for an activated contracted platelet. **f**, Platelets contracting in between fixed boundaries experience isometric contraction. Previous measurements in isometric contractile conditions found maximal forces of 80nN. **g**, Platelets pulling a fibrin strand perpendicular to the principle axis will cause minimal extension of the fibrin, exerting single nanonewton forces. **h**, Platelets which extend a single fibrin fiber will need to exert several 10s of nanonewtons. Neither g nor h consider pre-strain in the fibrin or multiple fibers which will make the conditions much stiffer.



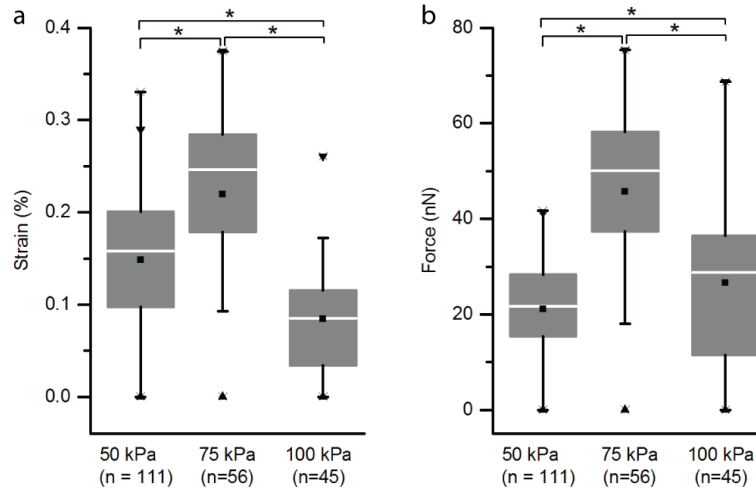
Supplementary Figure 3: Detailed process flow for construction of the platelet contraction cytometer. Due to the commercial availability of most starting materials, batches of devices may be made in less than 8 hours.



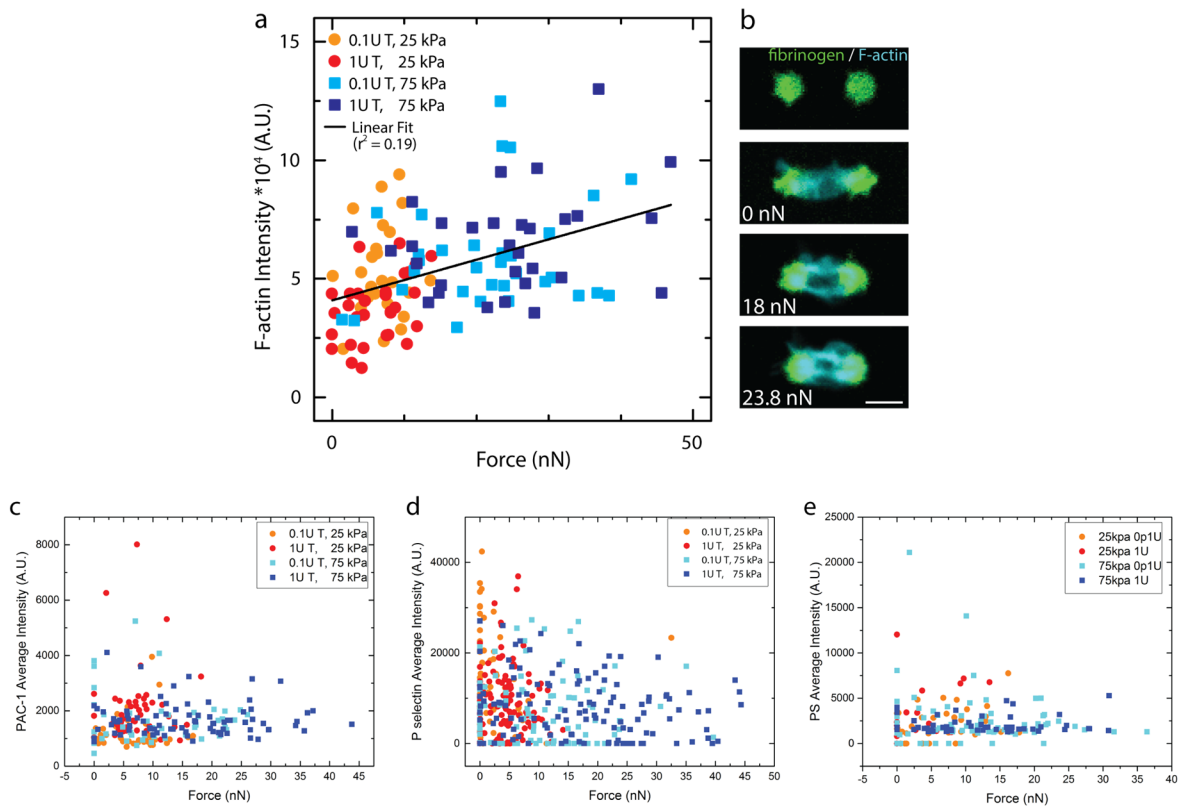
Supplementary Figure 4: Cast polyacrylamide gels in laser cut gaskets are equivalent to macro systems and enable independent measurements of platelet contractile forces. **a**, Measurements of polyacrylamide gels in channels demonstrate that gels are thicker than 70 μm to ensure that the underlying glass substrate does not contribute to the locally measured stiffness (n = 4, error bars show standard deviation). **b**, The measured stiffness values are in agreement with estimated values, and similar to previously published values in the literature. (n = 18 from two different gels, error bars show standard deviation) **c-d**, A single contracting platelet on a microdot pair does not affect the displacement of the surrounding microdot pairs, demonstrating that each microdot pair is independent from the neighbor.



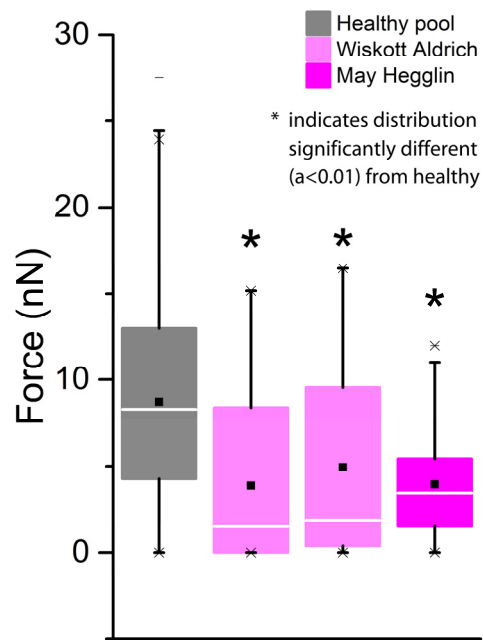
Supplementary Figure 5: Application of shear stress after the initiation of adhesion and contraction has no statistical change on platelet contractile forces. (a) Shear flow was applied at  $100 \text{ s}^{-1}$  with differing stiffness and thrombin concentration (b) Differing shear was applied at  $25 \text{ kPa}$  and  $1 \text{ U/mL}$  thrombin. ( $n_{\text{condition}} \geq 35$ ,  $n_{\text{total}} = 887$ )



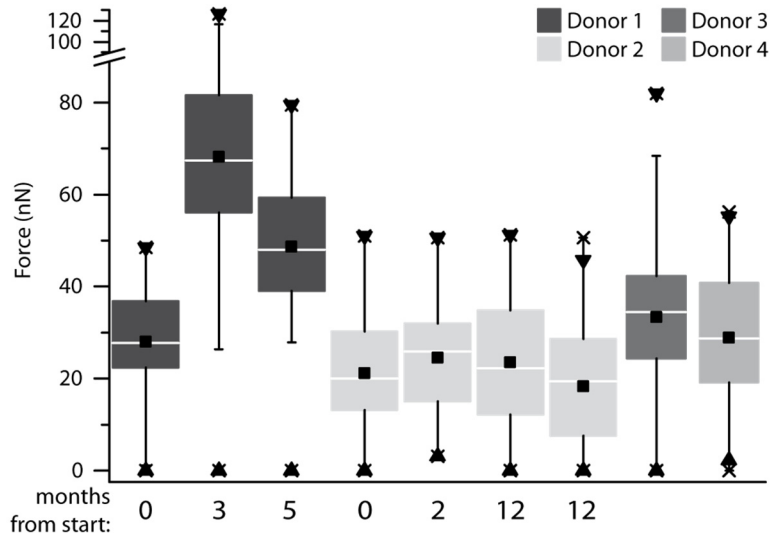
Supplementary Figure 6: Platelet microdot displacement and force is reduced as the environmental stiffness increases. **a**, Measured microdot displacements become small when the environmental stiffness is very high at 100 kPa. **b**, When converted to force, the distances measured in (a) reveal that a similar range of forces is seen between 75 kPa and 100 kPa stiffness gels, but that the average force is lower, indicating that on average platelets do not apply high contraction forces efficiently in very high stiffness environments. Significance by Mann-Whitney,  $\alpha < 0.05$ .



Supplementary Figure 7: F-actin intensity weakly correlates with platelet contractile force, and no discernable correlation is seen with other markers of platelet activation. **a**, F-actin content weakly correlates with contractile force in a variety of different thrombin and mechanical conditions. Correlation of  $r > 0.3$  at  $\alpha = 0.05$ . **b**, Selected images of a separate experiment with 0.1 U/mL thrombin and 25 kPa of some platelets showing increase and improved organization in F-actin with increasing contractile force. As indicated in **a**, there were also some platelets which did not follow this trend. Little to no correlation in force and **c**, PAC-1 binding, **d**, P-selectin binding, or **e**, PS exposure was observed.



Supplementary Figure 8: Platelet contractile forces are impaired in individuals with actomyosin related cytoskeletal mutations on soft (25 kPa) gels. ( $n_{\text{patient}} \geq 28$ ,  $n_{\text{total}} = 598$ )



Supplementary Figure 9: Platelet contraction for the same donor over time with numbers indicating time from start. Donor 1 and donor 2 defined the limits of the contraction range measured for healthy individuals, with donor 1 having a high variability in between measurements and donor 2 having exceptionally low variability in between measurements. Donors 3 and 4 were measured at a later time point in the study. ( $n_{\text{patient}} \geq 30$ ,  $n_{\text{total}} = 616$ )

Study ID	Contractile force	Bleeding history	Plt count (10 <sup>3</sup> /uL)	PT (s)	aPTT (s)	fibrinogen (mg/dL)	Factor VIII assay (%)	VWF Ag (%)	Ristocetin cofactor	thrombin time (s)
WL05		easy bruising, spontaneous hematomas, hematuria, occasional nosebleeds	210	13.5	30.6	307	137	107	107	16.8
WL02		heavy menstruation, easy bruising and gum bleeding	229	14	28.9	255	134	96	62	14.9
WL06	low	frequent prolonged nosebleeds, gum bleeding	245	14.6	29.5	330	127	79	78	16.4
WL07	low	frequent nosebleeds	348	14.3	29.2	227	163	165	81	19.3
WL03	very low	heavy menstruation, easy bruising, frequent gum bleeding and nosebleeds	240	13.3	29.9	343	183	60	54	16.4

0 Supplementary Table 1: Patient history and labs for individuals with unknown bleeding disorders

1

2

3

Study ID	Contractile force	Platelet aggregation interpretation by hematopathologist	PFA
WL05		normal platelet aggregation and release with ADP, arachadonic acid, collagen, ristocetin (low and high dose), thrombin	closure time with collagen/epi - 106 s (normal:83-163 s) and collagen/ADP - 73 s (normal:72-111 s)
WL02		normal platelet aggregation and release with ADP, arachadonic acid, collagen, ristocetin (low and high dose), thrombin	closure time with collagen/epi - 243 s (normal:83-163 s) and collagen/ADP - 174 s (normal:72-111 s) but Hct at 19.4
WL06	low	normal platelet aggregation and release with ADP, arachadonic acid, collagen, ristocetin (low and high dose), thrombin	closure time with collagen/epi - 116 s (normal:83-163 s) and collagen/ADP - not reported (normal:72-111 s)
WL07	low	Mildly decreased aggregation to low and high dose collagen, with normal ATP release. Given all other agonists are normal, this finding likely is clinically insignificant. Repeat testing may be performed if clinically indicated	closure time with collagen/epi - 107 s (normal:83-163 s) and collagen/ADP - 68 (normal:72-111 s)
WL03	very low	normal platelet aggregation and release with ADP, arachadonic acid, collagen, ristocetin (low and high dose), thrombin	closure time minimally elevated with collagen/epi - 177 s (normal:83-163 s) and collagen/ADP - 116 s (normal:72-111 s)

4

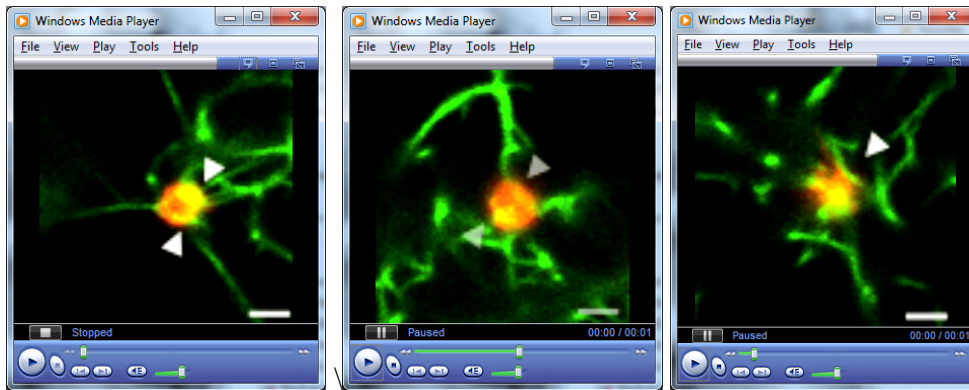
5 Supplementary Table 2: Interpretation of history and labs for individuals with unknown bleeding disorders by hemopathologist with

6 PFA data

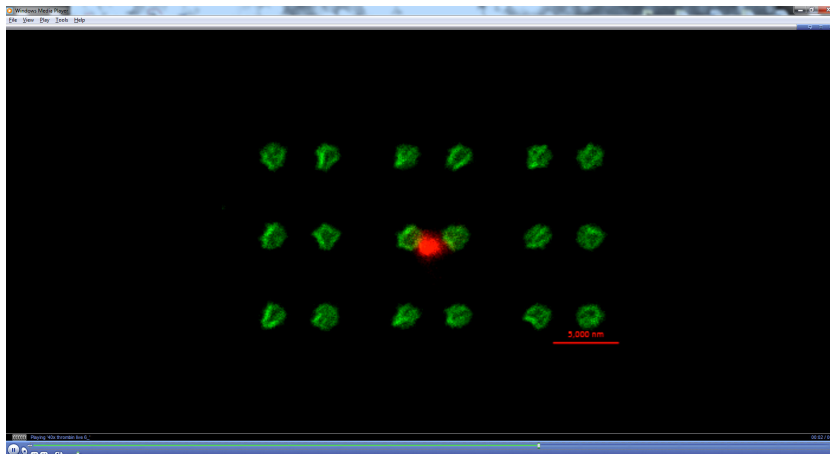
7

8

## Supplementary Videos



Supplementary Video 1-3: Platelet contraction in 3d fibrin meshes span and pull adjacent fibers together of differing stiffness. The fibrin mesh has varying mechanical stiffness due to the differing thickness and cross linking point density. Here we show three platelets spanning fibrin filaments and pulling them together over the course of six minutes. White arrows point to same feature at both time points. Scale bar is 2  $\mu\text{m}$ .



Supplementary Video 4: Individual contracting platelet - A single contracting platelet is imaged during the contraction process. Time elapsed for entire video is 60 minutes.